

Deformation of Λ hypernuclei

Myaing Thi Win and K. Hagino

Department of Physics, Tohoku University, Sendai 980-8578, Japan

(Dated: November 13, 2018)

We study the deformation property of Λ hypernuclei using the relativistic mean field (RMF) method. We find that ${}^{29}_{\Lambda}\text{Si}$ and ${}^{13}_{\Lambda}\text{C}$ hypernuclei have spherical shape as a consequence of the additional Λ particle, whereas the corresponding core nuclei, ${}^{28}\text{Si}$ and ${}^{12}\text{C}$, are oblatelly deformed. Most of other hypernuclei have a similar deformation parameter to the core nucleus, in accordance with the previous study with the non-relativistic Skyrme-Hartree-Fock method. We discuss the sensitivity of our results to the choice of pairing interaction and to the parameter set of the RMF Lagrangian.

PACS numbers: 21.80.+a, 21.10.Dr, 21.30.Fe, 21.60.Jz

I. INTRODUCTION

It has been well known that many open-shell nuclei are deformed in the ground state. The nuclear deformation generates the collective rotational motion, which is characterized by a pronounced rotational spectrum as well as strongly enhanced quadrupole transition probabilities. Theoretically, a standard way to discuss nuclear deformation is a self-consistent mean-field theory [1]. By allowing the rotational symmetry to be broken in the mean-field potential, the mean-field theory provides an intuitive and transparent view of the nuclear deformation. See *e.g.*, Ref. [2] for a recent systematic study of nuclear deformation based on the Skyrme-Hartree-Fock-Bogoliubov method. The state-of-the-art mean-field approach also takes into account the effects beyond the mean-field approximation, such as the angular momentum projection and the configuration mixing [3].

The self-consistent mean-field method has been extensively applied also to hypernuclei [4, 5, 6, 7, 8, 9, 10, 11, 12, 13, 14, 15, 16, 17, 18, 19] (see Ref. [20] for a recent experimental review on Λ hypernuclei). These calculations have successfully reproduced the mass number dependence of Λ binding energy, from a light nucleus ${}^{12}_{\Lambda}\text{C}$ to a heavy nucleus ${}^{208}_{\Lambda}\text{Pb}$. We notice that most of these calculations have assumed spherical symmetry. Only recently, deformed calculations have been carried out in a broad mass region using the non-relativistic Skyrme Hartree-Fock method [11]. The authors of Ref. [11] have reported that the hypernuclei which they studied have a similar deformation parameter to the corresponding core nuclei with the same sign.

The aim of this paper is to study the deformation property of Λ hypernuclei using the relativistic mean field (RMF) method, as an alternative choice of effective NN and $N\Lambda$ interactions. The RMF method has been as successful as the Skyrme-Hartree-Fock method in describing stable nuclei as well as nuclei far from the stability line [21, 22]. Vretenar *et al.* have argued [17] that the change in the nucleon spin-orbit potential due to the presence of Λ particle is much more emphasized in the RMF approach as compared to the non-relativistic approach, since the spin-orbit potential in the former ap-

proach is actually given as a sum of scalar and vector potentials. That is, even if the change in the mean-field potential (given as a difference of scalar and vector potentials) is small, the change in the spin-orbit potential may not necessarily be small. Therefore, a slightly different conclusion from that with the non-relativistic approach may result concerning the structure of hypernuclei. In fact, we will demonstrate below that the shape of ${}^{12}\text{C}$ and ${}^{28}\text{Si}$ nuclei are drastically changed when a Λ particle is added to them.

The paper is organised as follows. In Sec. II, we briefly summarize the RMF approach for Λ hypernuclei. In Sec. III, we apply the RMF method to Ne and Si isotopes, and discuss the influence of Λ particle on the deformation of the hypernuclei. We also discuss the deformation of ${}^{12}\text{C}$ and ${}^{13}_{\Lambda}\text{C}$ nuclei. We summarize the paper in Sec. IV.

II. RMF FOR Λ HYPERNUCLEI

In the RMF approach, nucleons and a Λ particle are treated as structureless Dirac particles, interacting through the exchange of virtual mesons, that is, the isoscalar scalar σ meson, the isoscalar vector ω meson, and the isovector vector ρ meson. The photon field is also taken into account to describe the Coulomb interaction between protons. The effective Lagrangian for Λ hypernuclei may be given as [12, 13, 14, 15, 16, 17, 18, 19]

$$\mathcal{L} = \mathcal{L}_N + \bar{\psi}_{\Lambda} [\gamma_{\mu} (i\partial^{\mu} - g_{\omega\Lambda}\omega^{\mu}) - m_{\Lambda} - g_{\sigma\Lambda}\sigma] \psi_{\Lambda}, \quad (1)$$

where ψ_{Λ} and m_{Λ} are the Dirac spinor and the mass for the Λ particle, respectively. Notice that the Λ particle couples only to the σ and ω mesons, as it is neutral and isoscalar. Those coupling constants are denoted as $g_{\sigma\Lambda}$ and $g_{\omega\Lambda}$, respectively. For simplicity, we neglect the tensor Λ - ω interaction. This is justified since we consider only the ground state configuration, in which the Λ particle occupies the lowest $K^{\pi} = 1/2^{+}$ single-particle state [16, 17], K being the projection of the single-particle angular momentum onto the symmetry axis. \mathcal{L}_N in Eq. (1) is the standard RMF Lagrangian for the nucleons. See *e.g.*, Refs. [17, 21, 22] for its explicit form.

We solve the RMF Lagrangian (1) in the mean field approximation. The variational principle leads to the Dirac equation for the Λ particle,

$$[-i\boldsymbol{\alpha} \cdot \boldsymbol{\nabla} + \beta(m_\Lambda + g_{\sigma\Lambda}\sigma(\mathbf{r})) + g_{\omega\Lambda}\omega^0(\mathbf{r})] \psi_\Lambda = \epsilon_\Lambda \psi_\Lambda, \quad (2)$$

where ϵ_Λ is the single-particle energy for the Λ particle state, and the Klein-Gordon equation for the mesons,

$$[-\nabla^2 + m_\sigma^2]\sigma(\mathbf{r}) = -g_\sigma\rho_s(\mathbf{r}) - g_2\sigma(\mathbf{r})^2 - g_3\sigma(\mathbf{r})^3 - g_{\sigma\Lambda}\psi_\Lambda^\dagger(\mathbf{r})\gamma^0\psi_\Lambda(\mathbf{r}), \quad (3)$$

$$[-\nabla^2 + m_\omega^2]\omega^0(\mathbf{r}) = g_\omega\rho_v(\mathbf{r}) + g_{\omega\Lambda}\psi_\Lambda^\dagger(\mathbf{r})\psi_\Lambda(\mathbf{r}). \quad (4)$$

To derive these equations, we have used the time-reversal symmetry and retained only the time-like component of ω^μ [21]. ρ_s and ρ_v are the scalar and vector densities for the nucleons, which are constructed with the spinor for the nucleons using the so called no-sea approximation, *i.e.*, neglecting the contribution from the antiparticles. g_σ and g_ω are the coupling constants of the nucleons to the sigma and the omega mesons, respectively, and g_2 and g_3 are the coefficients in the non-linear sigma terms in \mathcal{L}_N .

We solve these equations, together with the Dirac equation for the nucleons and the Klein-Gordon equations for the ρ meson and the photon field, iteratively until the self-consistency condition is achieved. For this purpose, we modify the computer code RMFAXIAL [23] to include the Λ particle. In this code, the RMF equations for the nucleons are solved with the harmonic oscillator expansion method[21], assuming the axial symmetry. The pairing correlation among the nucleons is also taken into account in the BCS approximation.

With the self-consistent solution of the RMF equations, we compute the intrinsic quadrupole moment of the hypernucleus,

$$Q = \sqrt{\frac{16\pi}{5}} \int d\mathbf{r} [\rho_v(\mathbf{r}) + \psi_\Lambda^\dagger(\mathbf{r})\psi_\Lambda(\mathbf{r})] r^2 Y_{20}(\hat{\mathbf{r}}). \quad (5)$$

The quadrupole deformation parameter β_2 is then estimated with the intrinsic quadrupole moment as [21, 24, 25],

$$Q = \sqrt{\frac{16\pi}{5}} \frac{3}{4\pi} (A_c + 1) R_0^2 \beta_2, \quad (6)$$

where $A_c = A - 1$ is the mass number of the core nucleus for the hypernucleus. We use $R_0 = 1.2A_c^{1/3}$ fm for the radius of the hypernucleus.

III. QUADRUPOLE DEFORMATION OF Λ HYPERNUCLEI

We now numerically solve the RMF equations and discuss the quadrupole deformation parameter of Λ hypernuclei. For this purpose, we use the NL3 parameter

set[26] for the RMF Lagrangian for the nucleons, \mathcal{L}_N . For the Λ -meson coupling constants, we follow Refs. [15, 17] and take $g_{\omega\Lambda} = \frac{2}{3}g_\omega$ and $g_{\sigma\Lambda} = 0.621g_\sigma$. The value for $g_{\omega\Lambda}$ was determined from the naive quark model [16], while the value for $g_{\sigma\Lambda}$ was slightly fine-tuned in order to reproduce the Λ binding energy of $^{17}_\Lambda\text{O}$ [15]. For the pairing correlation among the nucleons, we employ the constant gap approximation with the pairing gap given in Ref. [27], that is, $\Delta_n = 4.8/N^{1/3}$ and $\Delta_p = 4.8/Z^{1/3}$ MeV for the neutron and the proton pairing gaps, respectively. (It has been known that these pairing gaps underestimate the deformation parameter of ^{20}Ne nucleus when it is calculated with the NL3 parameter set[28, 29]. We therefore arbitrarily switch off the pairing interaction when we calculate the ^{20}Ne and $^{21}_\Lambda\text{Ne}$ nuclei.)

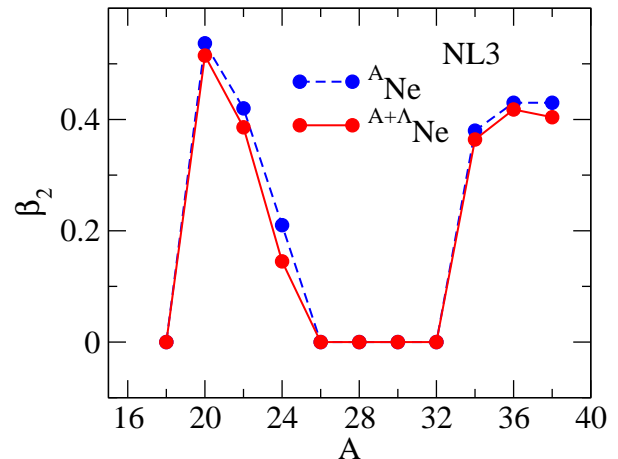


FIG. 1: (Color online) Quadrupole deformation parameter for Ne isotopes obtained with the RMF method with the NL3 parameter set. The dashed line is the deformation parameter for the core nucleus, while the solid line is for the corresponding hypernucleus.

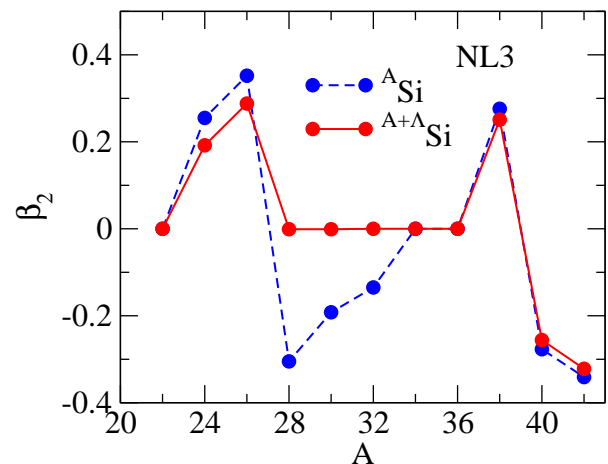


FIG. 2: (Color online) Same as Fig.1, but for Si isotopes.

Figures 1 and 2 show the deformation parameter for the ground state of Ne and Si isotopes, respectively. The dashed line is the deformation parameter for the even-even core nuclei, while the solid line is for the corresponding hypernuclei. For the Ne isotopes, the deformation parameter is always similar between the core nucleus and the corresponding hypernucleus, although the deformation parameter for the hypernucleus is slightly smaller than that for the core nucleus. This is consistent with the previous results with the non-relativistic Skyrme-Hartree-Fock method [11]. On the other hand, for the Si isotopes, the deformation parameter for the $^{28,30,32}\text{Si}$ nuclei is drastically changed when a Λ particle is added, although the change for the other Si isotopes is small. That is, the $^{28,30,32}\text{Si}$ nuclei have oblate shape in the ground state. When a Λ particle is added to these nuclei, remarkably they turn to be spherical.

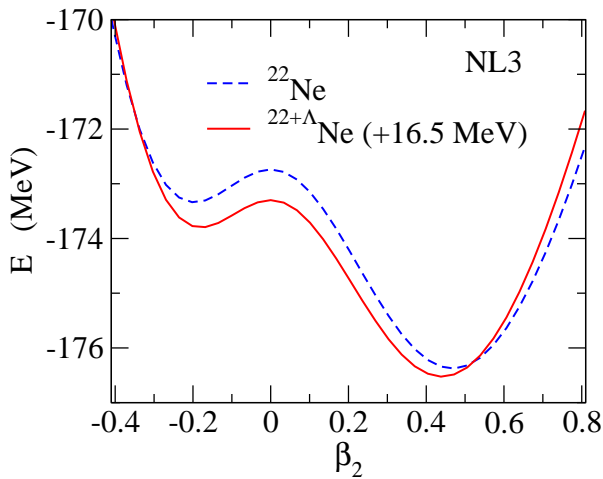


FIG. 3: (Color online) The potential energy surface for the ^{22}Ne (the dashed line) and $^{22+\Lambda}\text{Ne}$ (the solid line) nuclei obtained with the constrained RMF method with the NL3 parameter set. The energy surface for $^{22+\Lambda}\text{Ne}$ is shifted by a constant amount as indicated in the inset.

The potential energy surfaces for the $^{22,22+\Lambda}\text{Ne}$ and $^{28,28+\Lambda}\text{Si}$ nuclei are shown in Figs. 3 and 4, respectively. These are obtained with the constrained RMF method with quadrupole constraint [24, 30]. The meaning of each line is the same as in Figs. 1 and 2. In order to facilitate the comparison, we shift the energy surface for the hypernuclei by a constant amount as indicated in the inset of the figures. For the ^{22}Ne nucleus, the prolate minimum in the energy surface is relatively deep (the energy difference between the oblate and the prolate minima is 3.04 MeV, and that between the spherical and prolate configurations is 3.63 MeV), and it is affected little by the addition of the Λ particle. On the other hand, the energy surface for the ^{28}Si nucleus shows a relatively shallow oblate minimum, with a shoulder at the spherical configuration. The energy difference between the oblate and the spherical configurations is 0.754 MeV, and could be easily inverted when a Λ particle is added.

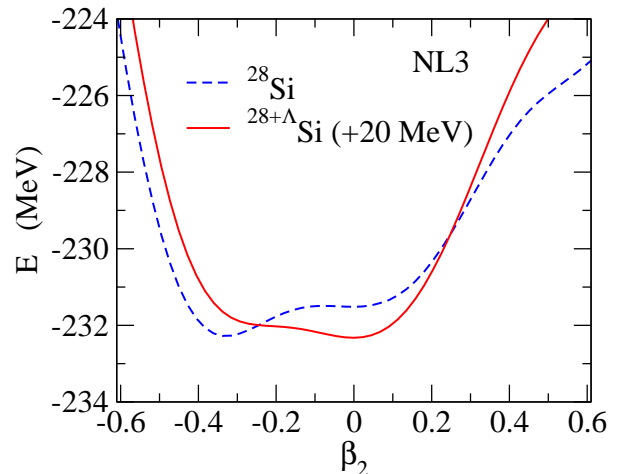


FIG. 4: (Color online) Same as Fig. 3, but for the ^{28}Si and $^{28+\Lambda}\text{Si}$ nuclei.

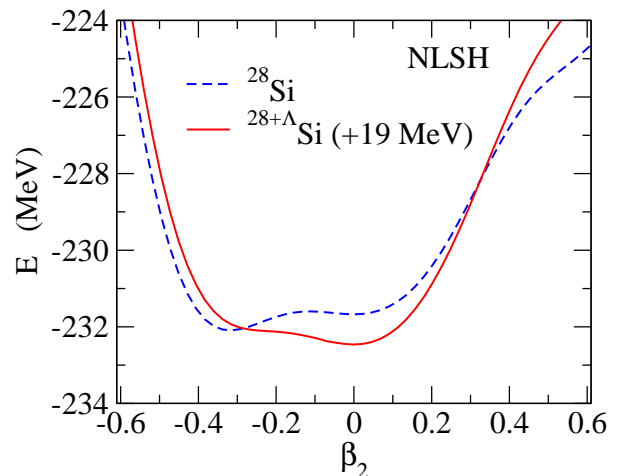


FIG. 5: (Color online) Same as Fig. 4, but obtained with the NLSH parameter set.

In order to check the parameter set dependence of the results, we repeat the same calculation with the NLSH parameter set [31]. The potential energy surface for the $^{28,28+\Lambda}\text{Si}$ nuclei obtained with the NLSH set is shown in Fig. 5. One sees that the potential energy surface is qualitatively almost the same between the NL3 and NLSH parameter sets, although the Λ binding energy is slightly different. Namely, the oblate ^{28}Si nucleus becomes spherical in the presence of Λ particle, again with the NLSH parameter set. We also check the dependence of the results on the treatment of pairing correlation. For this purpose, we perform the calculations i) without taking into account the pairing correlation and ii) with the constant force approach for the strength of the seniority pairing force. For the latter approach, we determine G_p and G_n so that they lead to $\Delta_n = 4.8/N^{1/3}$ and $\Delta_p = 4.8/Z^{1/3}$ MeV for the ground state of each nucleus.

(For instance, $G_p = 17.38/A$ and $G_n = 15.97/A$ MeV for the NL3 calculation of ^{28}Si nucleus.) We confirm that our conclusion remains the same for both the treatments of the pairing correlation, due to the fact that N or $Z=14$ is an oblate magic number[32]. We therefore conclude that the Λ particle significantly changes the deformation of ^{28}Si nucleus, at least for the two parameter sets of the RMF Lagrangian and irrespective of the treatment of pairing correlations.

In contrast, for the $^{30,32}\text{Si}$ nuclei, the dependence on the parameter set and the treatment of pairing is much stronger. For instance, with the NLSH parameter set, the $^{30+\Lambda}\text{Si}$ is slightly oblate and the deformation parameter is similar between ^{32}Si and $^{32+\Lambda}\text{Si}$. Without the pairing correlation, the deformation is similar between ^{32}Si and $^{32+\Lambda}\text{Si}$ for both NL3 and NLSH. Apparently more careful investigations will be necessary for these nuclei before we can draw a definite conclusion on their deformation parameter. We summarize our results for $^{28,30,32}\text{Si}$ and $^{28,30,32}\text{Si} + \Lambda$ in Table I.

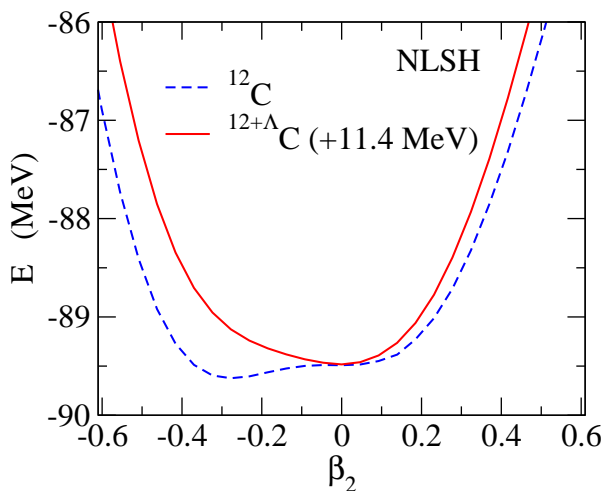


FIG. 6: (Color online) Same as Fig. 5, but for the ^{12}C and $^{12+\Lambda}\text{C}$ nuclei.

As another example which shows a large effect of Λ particle on nuclear deformation, we next discuss the ^{12}C nucleus. For this nucleus, the calculation with the NL3 parameter set did not converge, due to the instability of the scalar meson field [33, 34], and we here show only the results with the NLSH set. Fig. 6 shows the potential energy surface obtained with the NLSH parameter set together with the constant gap approximation for the pairing correlation. The behaviour of energy surface of ^{12}C is similar to that of ^{28}Si shown in Figs. 4 and 5.

That is, the energy surface has a shallow oblate minimum and a shoulder at the spherical configuration. For this nucleus, the energy difference between the oblate and the spherical configurations is as small as 0.13 MeV. By adding a Λ particle, the oblate minimum disappears and the ground state becomes spherical. This is exactly the same effect of Λ particle as that in the ^{28}Si nucleus. For this light nucleus, the pairing correlation does not play an essential role, and we confirm that our conclusion remains the same even if we do not include the pairing correlation (see Table I).

IV. SUMMARY

We have used the relativistic mean field (RMF) theory to investigate quadrupole deformation of Λ hypernuclei. We have shown that, while an addition of Λ particle does not influence much the shape of many nuclei, ^{12}C and ^{28}Si make important exceptions. That is, we have demonstrated that the Λ particle makes the shape of these nuclei change from oblate to spherical. For the ^{28}Si nucleus, this conclusion was achieved both with the NL3 and NLSH parameter sets of the RMF Lagrangian, although the calculation with NL3 was not converged for the ^{12}C nucleus due to the instability of sigma field. We have also confirmed that the conclusion is independent of the treatment of pairing correlation among the nucleons.

An important next question will be how to observe experimentally the drastic structure change of the hypernuclei found in this paper. For this purpose, a measurement of the energy of the first 4^+ state, and thus a deviation from a rotational spectrum, will be extremely useful. On the other hand, the potential energy surface for the $^{13}_{\Lambda}\text{C}$ and $^{29}_{\Lambda}\text{Si}$ nuclei is somewhat soft and a large anharmonic effect of collective vibration might be expected. One may thus need to perform *e.g.*, a generator coordinate method (GCM) calculation [3], on top of the mean field calculation presented in this paper, and calculate the excitation spectra before one can compare the theoretical results with experimental data.

Acknowledgments

We thank H. Tamura, H. Sagawa, Nyein Wink Lwin, and Khin Nyan Linn for useful discussions. This work was supported by the Japanese Ministry of Education, Culture, Sports, Science and Technology by Grant-in-Aid for Scientific Research under the program number 19740115.

-
- [1] M. Bender, P.H. Heenen, and P.-G. Reinhard, Rev. Mod. Phys. **75**, 121 (2003).
 [2] M.V. Stoitsov, J. Dobaczewski, W. Nazarewicz, S. Pittel,

- and D.J. Dean, Phys. Rev. C **68**, 054312 (2003).
 [3] M. Bender and P.H. Heenen, Phys. Rev. C, in press, and references therein. arXiv:0805.4383 [nucl-th].

TABLE I: Comparison of deformation parameter for the $^{28,30,32}\text{Si}$, $^{28,30,32+\Lambda}\text{Si}$, and $^{12,12+\Lambda}\text{C}$ nuclei obtained with the NL3 and NLSH parameter sets of RMF Lagrangian. The pairing correlation is taken into account either in the constant Δ (*i.e.*, constant pairing gap) or in the constant G (*i.e.*, constant pairing force) approximations for a seniority pairing interaction. The results without the pairing correlation are also shown. The calculation with the NL3 set did not converge for $^{12,12+\Lambda}\text{C}$ and the results are not shown in the table.

nucleus	NL3			NLSH		
	const.- Δ	const.- G	no-pairing	const.- Δ	const.- G	no-pairing
^{28}Si	-0.31	-0.29	-0.33	-0.29	-0.25	-0.32
$^{28+\Lambda}\text{Si}$	0.00	0.01	0.00	0.00	0.00	0.00
^{30}Si	-0.19	-0.19	0.15	-0.19	-0.19	0.19
$^{30+\Lambda}\text{Si}$	0.00	0.00	0.00	-0.06	0.06	0.18
^{32}Si	-0.14	-0.14	-0.20	-0.15	-0.15	-0.20
$^{32+\Lambda}\text{Si}$	0.00	-0.00	-0.18	-0.11	0.12	-0.18
^{12}C				-0.25	-0.25	-0.286
$^{12+\Lambda}\text{C}$				0.00	0.00	0.00

- [4] M. Rayet, Nucl. Phys. **A367**, 381 (1981).
- [5] Y. Yamamoto, H. Bandō, and J. Zofka, Prog. Theo. Phys. **80**, 757.
- [6] Y. Yamamoto and H. Bandō, Prog. Theo. Phys. **83**, 254 (1990).
- [7] D.E. Lanskoy and Y. Yamamoto, Phys. Rev. **C55**, 2330(1997).
- [8] D.E. Lanskoy, Phys. Rev. **C58**, 3351 (1998).
- [9] J. Cugnon, A. Lejeune, and H.-J. Schulze, Phys. Rev. **C62**, 064308 (2000).
- [10] I. Vidaña, A. Polls, A. Ramos, and H.-J. Schulze, Phys. Rev. **C64**, 044301 (2001).
- [11] X.-R. Zhou, H.-J. Schulze, H. Sagawa, C.-X. Wu, and E.-G. Zhao, Phys. Rev. **C76**, 034312 (2007).
- [12] J. Mares and J. Zofka, Z. Phys. **A333**, 209 (1989); *ibid*, **A345**, 47 (1993).
- [13] M. Rufa, J. Schaffner, J. Maruhn, H. Stöcker, W. Greiner, and P.-G. Reinhard, Phys. Rev. **C42**, 2469 (1990).
- [14] N.K. Glendenning, D. Von-Eiff, M. Haft, H. Lenske, and M.K. Weigel, Phys. Rev. **C48**, 889 (1993).
- [15] J. Mares and B.K. Jennings, Phys. Rev. **C49**, 2472 (1994).
- [16] Y. Sugahara and H. Toki, Prog. Theo. Phys. **92**, 803 (1994).
- [17] D. Vretenar, W. Pöschl, G.A. Lalazissis, and P. Ring, Phys. Rev. **C57**, R1060 (1998).
- [18] H.F. Lü, J. Meng, S.Q. Zhang, and S.-G. Zhou, Eur. Phys. J. **A17**, 19 (2003).
- [19] H. Shen, F. Yang, and H. Toki, Prog. Theo. Phys. **115**, 325 (2006).
- [20] O. Hashimoto and H. Tamura, Prog. Part. Nucl. Phys. **57**, 564 (2006).
- [21] Y.K. Gambhir, P. Ring, and A. Thimet, Ann. of Phys. (N.Y.), **198**, 132 (1990).
- [22] P. Ring, Prog. Part. Nucl. Phys. **37**, 193 (1996).
- [23] P. Ring, Y.K. Gambhir, and G.A. Lalazissis, Comp. Phys. Comm. **105**, 77 (1997).
- [24] P. Ring and P. Schuck, *The Nuclear Many Body Problem* (Springer-Verlag, New York, 1980).
- [25] K. Hagino, N.W. Lwin, and M. Yamagami, Phys. Rev. **C74**, 017310 (2006).
- [26] G.A. Lalazissis, D. Vretenar, and P. Ring, Phys. Rev **C55**, 540 (1997).
- [27] P. Möller and J.R. Nix, Nucl. Phys. **A536**, 20 (1992).
- [28] A. Bhagwat and Y.K. Gambhir, Phys. Rev. **C68**, 044301 (2003).
- [29] G.A. Lalazissis, S. Raman, and P. Ring, At. Data Nucl. Data Tables **71**, 1 (1999).
- [30] H. Flocard, P. Quentin, A.K. Kerman, and D. Vautherin, Nucl. Phys. **A203**, 433 (1973).
- [31] M.M. Sharma, M.A. Nagarajan, and P. Ring, Phys. Lett. **B312**, 377 (1993).
- [32] I. Ragnarsson, S.G. Nilsson, and R.K. Sheline, Phys. Rep. **45**, 1 (1978).
- [33] P.-G. Reinhard, Z. Phys. **A329**, 257 (1988).
- [34] J. Fink, V. Blum, P.-G. Reinhard, J.A. Maruhn, and W. Greiner, Phys. Lett. **B218**, 277 (1989).